eNeuro

Research Article: New Research | Cognition and Behavior

Multi-scale Imaging Reveals Aberrant Functional Connectome Organization and Elevated Dorsal Striatal *Arc* Expression in Advanced Age

https://doi.org/10.1523/ENEURO.0047-19.2019

Cite as: eNeuro 2019; 10.1523/ENEURO.0047-19.2019

Received: 6 February 2019
Revised: 30 November 2019
Accepted: 5 December 2019

1. Manuscript Title: Multi-scale Imaging Reveals Aberrant Functional Connectome Organization and Elevated Dorsal Striatal *Arc* Expression in Advanced Age

2. Abbreviated Title: Aberrant connectome organization and elevated *Arc*

3. Luis M. Colon-Perez[1], Sean M. Turner[3], Katelyn N. Lubke[3], Marjory Pompilus[2], Marcelo Febo[2-4*], and Sara N. Burke[3,4*]

Department of Neurobiology and Behavior, University of California, Irvine[1], Departments of Psychiatry[2], and Neuroscience [3], McKnight Brain Institute and College of Medicine[4], University of Florida, Gainesville, FL, 32610 USA

4. Author Contributions: LMC performed research, contributed analytic tools, analyzed data, and wrote the paper; SMT performed research and analyzed data; KNL performed research and analyzed data; MP performed research and assisted with analysis; MF designed research, performed research, contributed analytic tools, and analyzed data; SNB designed research, performed research, contributed analytic tools, analyzed data and wrote the paper.

5. Correspondence should be addressed to:
*Indicates shared corresponding authorship
Sara N. Burke, PhD, Department of Neuroscience, University of Florida, P.O. Box 100244, Gainesville, FL 32611; Tel. +1 (352) 294-4979; Fax: +1 (352) 392-8347; Email: burkes@ufl.edu
Marcelo Febo, PhD, Department of Psychiatry, University of Florida, P.O. Box 100256, Gainesville, FL 32610; Tel. +1 (352) 294-4911; Fax: +1 (352) 392-8217; Email: febo@ufl.edu

6. Number of Figures: 11
7. Number of Tables: 2
8. Number of Multimedia: 0
9. Number of words for Abstract: 226
10. Number of words for Significance Statement: 120
11. Number of words for Introduction: 718
12. Number of words for Discussion: 1859

13. Acknowledgements:
The authors would like to acknowledge Michael G. Burke for constructing the behavioral apparatus and Dr. Andrew P. Maurer for the helpful discussions during the preparation of this manuscript.

14. Conflict of Interest
A. Authors report no conflict of interest.

15. Funding sources:
This work was supported by National Institutes of Health National Institute on Aging grants R01 AG049722 and P50 AG047266, and the McKnight Brain Research Foundation. The authors acknowledge the support from the Advanced Magnetic Resonance Imaging and Spectroscopy (AMRIS) facility (National Science Foundation Cooperative Agreement No. DMR-1157490 and the State of Florida).

ABSTRACT

The functional connectome reflects a network architecture enabling adaptive behavior that becomes vulnerable in advanced age. The cellular mechanisms that contribute to altered functional connectivity in old age, however, are not known. Here we used a multi-scale imaging approach to link age-related changes in the functional connectome to altered expression of the activity-dependent immediate-early gene *Arc* as a function of training to multi-task on a working memory/bi-conditional association task (WM/BAT). Resting state fMRI data were collected from young and aged rats longitudinally at three different timepoints during cognitive training. After imaging, rats performed the WM/BAT and were immediately sacrificed to examine expression levels of *Arc* during task performance. Aged behaviorally-impaired, but not young, rats had a subnetwork of increased connectivity between the anterior cingulate cortex (ACC) and dorsal striatum (DS) that was correlated with the use of a suboptimal response-based strategy during cognitive testing. Moreover, while young rats had stable rich club organization across three scanning sessions, the rich club organization of old rats increased with cognitive training. In a control group of young and aged rats that were longitudinally scanned at similar time intervals, but without cognitive training, ACC-DS connectivity and rich club organization did not change between scans in either age group. These findings suggest that aberrant large-scale functional connectivity in aged animals is associated with altered cellular activity patterns within individual brain regions.

Key words: anterior cingulate cortex, functional connectivity, graph theory, prefrontal cortex, working memory

SIGNIFICANCE STATEMENT

Cognitive decline is frequently observed in advanced age. Although impairments in older adults have been linked to alterations in resting state brain connectivity, how these changes relate to the neurobiology of individual neurons is unknown. The current study reports longitudinal changes in the functional connectome of aged rats with cognitive training that were not observed in young animals with better task performance. These network alterations in old age were associated with poorer task performance and increased *Arc* expression in the dorsal striatum. This work is significant because it links functional organization of brain networks to behavioral impairments and changes within individual neurons, providing a potential bridge between invasive cell-based analyses in animal models to imaging data from human study participants.

INTRODUCTION

Advancing age is associated with cognitive impairments that can erode one's quality of life (Samson and Barnes, 2013; Lockhart and DeCarli, 2014). Behaviors that rely on interactions across brain networks, such as episodic memory and cognitive multi-tasking, appear to be particularly vulnerable to decline in older adults (Chadick et al., 2014; Fandakova et al., 2014) and animal models of aging (Hernandez et al., 2015; Gray et al., 2017). A possible reason for these cognitive impairments could be aberrant organization of the functional connectome with advancing age (Ash and Rapp, 2014; Sala-Llonch et al., 2014; Nyberg, 2017), which include decreased connectivity within the default mode network (Sala-Llonch et al., 2015a; Grady et al., 2016), increased functional connectivity within the hippocampal network (Salami et al., 2014), decreased segregation between different functional networks (Chan et al., 2014; Geerligs et al., 2014), as well as increased connectivity between the anterior cingulate cortex and other cortical structures (Cao et al., 2014b). Although it is unclear how different functional networks observed in humans map onto rodents, altered resting state functional connectivity has also been reported for old rats (Ash et al., 2016) and middle-aged mice (Egimendia et al., 2019), indicating that there is a cross-species consensus regarding the vulnerability of brain-wide networks to advancing age.

While altered network connectivity in older adults is thought to reflect neural inefficiency or dedifferentiation (Salami et al., 2014; Sala-Llonch et al., 2015b; Grady et al., 2016; Nyberg, 2017), it remains unclear how network parameters used to quantify large-scale functional connectome organization relate to age-associated neurobiological changes at the cellular level. Recent behavioral models for probing the integrity of inter-regional communication (Hernandez et al., 2015; Hernandez et al., 2017), along with advances in small animal functional MRI (Ash et al., 2016; Colon-Perez et al., 2016a) offer a unique opportunity to interrogate both large-scale functional connectome organization and cellular mechanisms of cognitive aging within the same

110 animals, providing a critical translational link to noninvasive imaging in human study
111 participants.

112 An additional advantage to working with animal models is the ability to longitudinally
113 measure resting state metrics of network architecture as a function of cognitive training in
114 populations with highly controlled dietary and behavioral experiences across age groups. While
115 working memory training in young adults (Takeuchi et al., 2017) and water maze training in
116 young rats (Nasrallah et al., 2016) has been shown to alter functional connectivity, it is unknown
117 whether cognitive training similarly impacts functional network architecture in aged populations.

118 The current study aimed to examine how cognitive training on a cognitive dual task,
119 which required animals to perform a spatial working memory and a biconditional association
120 task (WM/BAT) simultaneously, altered resting-state functional connectivity in young and aged
121 rats. This behavioral paradigm is known to require interactions between prefrontal, medial
122 temporal and subcortical structures (Jo and Lee, 2010; Hernandez et al., 2017), and is
123 vulnerable to decline in old age prior to the emergence of deficits on the hippocampus-
124 dependent Morris water maze (Hernandez et al., 2015). Rats were scanned at three time points
125 to measure longitudinal changes in brain connectivity during learning using graph theoretical
126 analysis. The rich club coefficient was included as an unbiased metric of network organization.
127 The rich club refers to a set of densely and highly inter-connected nodes known as hub regions
128 in the brain. Rich-club organization is an expensive network structure (i.e., extensive
129 connectivity and metabolic cost) that allows complex network dynamics to increase efficiency
130 (Kaiser and Hilgetag, 2006; van den Heuvel et al., 2012). In the context of functional networks,
131 the rich club describes an increase in participation and activation of certain active nodes into
132 members of a functional rich club (Liang et al., 2018). Importantly, rich club of connector hubs
133 are believed to be more vulnerable to damage in aging due to their metabolic demands
134 (Bullmore and Sporns, 2012; Hernandez et al., 2018b).

135 Following the last resting state scan, rats were assessed for the expression of the

activity-dependent immediate-early gene *Arc* (Cole et al., 1989; Guzowski et al., 1999) during WM/BAT behavior to directly relate neuronal activity during the task to network connectivity patterns obtained from resting state fMRI. Thus, the current experiments used a multi-scale imaging approach that spanned from single cells to global networks and behavior to explore neural network dynamics in young and old rats in relation to cognitive training.

MATERIALS AND METHODS

Subjects and behavioral testing. A total of 18 young (4 months old) and 22 aged (24 months old) male Fischer 344 x Brown Norway F1 (FBN) hybrid rats from the National Institute on Aging colony at Taconic Farms were used in this study. Rats were used across different cognitive training and imaging procedures and the sample size for each are summarized in Table 1. Notably, the lifespan of the FBN is greater than inbred Fisher 344 rats (Turturro et al., 1999), and many of the physical issues experienced by Fischer 344 rats are not evident in the FBN rats until they are older than 28 months (McQuail and Nicolle, 2015). Therefore, changes in performance are likely due to cognitive decline and not age-related physical impairment. A subset of five rats in each age group were shaped to run on the continuous-T maze for reward and then scanned for the network analysis at three different timepoints in relation to cognitive training on the WM/BAT. After scanning, these same rats were trained on a new WM/BAT problem set and then sacrificed to analyze *Arc* expression. For the *Arc* experiment, a new set of objects was used for WM/BAT because we wanted a similar time interval to pass between the final resting state scan and the *Arc* experiment as was separating the 3 resting state scans. Given that aged rats will eventually learn the WM/BAT problem (Hernandez et al., 2015; Hernandez et al., 2018b), we selected new objects to ensure that there would still be an age-related difference in task performance after an additional 2 weeks of testing.

One aged rat reached a humane endpoint prior to the *Arc* catFISH experiment and was therefore not included in the *Arc* expression analysis, but this animal's data were included in the

resting state analysis. An additional young (n = 1) and aged (n = 1) rat were sacrificed directly from the home cages as a negative control to ensure that nothing unexpected occurred in the colony room on the day of the experiment to increase *Arc* expression. Expression levels in these rats was low (<5% for anterior cingulate cortex and <2% for dorsal striatum; data not shown). To replicate the observation of elevated *Arc* expression in the dorsal striatum, a group of n = 7 young and n = 8 aged rats were trained on WM/BAT for 2 weeks and then were directly sacrificed following behavior to label *Arc* mRNA in the striatum. A final group of rats (n = 5 young and n = 8 aged) were trained to traverse a track for food reward without cognitive training and scanned longitudinally at similar time intervals to the rats that were cognitively trained on WM/BAT (baseline, at 11 days, and at 24 days). These animals served as controls to quantify the longitudinal stability of the functional connectome in the absence of cognitive training. Each rat was housed individually in a temperature and humidity-controlled vivarium and maintained on a reverse 12-hour light/dark cycle. All behavioral testing and scanning were performed in the dark phase.

Table 1: Animal number across different experimental groups and procedures

Rat Number	Experimental Procedures
n = 5 young; n = 5 aged*	Resting state functional MRI with cognitive training on WM/BAT, and *Arc* expression analysis. *1 aged rat was not included in the *Arc* analysis.
n = 7 young; n = 8 aged	WM/BAT training and *Arc* expression analysis only.
n = 5 young; n = 8 aged	Control rats with no cognitive training, continuous-T maze training and longitudinal resting state scans only.

All rats were allowed 1 week to acclimate to the housing facility prior to food restriction and initial behavioral shaping. One week after arrival, all rats were placed on restricted feeding in which 20.5 g (1.9 kcal/g) of moist chow was provided daily, and drinking water was provided *ad libitum*. Shaping began once rats reached approximately 85% of their baseline weights. Baseline weight was considered the weight at which an animal had an optimal body condition score of 3 (with 5 being obese). Throughout the period of restricted feeding, rats were weighed

daily, and body condition was assessed and recorded weekly to ensure a range of 2.5-3. The body condition score was assigned based on the presence of palpable fat deposits over the lumbar vertebrae and pelvic bones. Rats with a score under 2.5 were given additional food to promote weight gain. All procedures were in accordance with the National Institutes of Health Guide for the Care and Use of Laboratory Animals and approved by the Institutional Animal Care and Use Committee.

Once rats reached 85% of their baseline weight, after ~1 week of restriction, they began shaping on the WM/BAT track. Rats were first habituated to the testing apparatus for 10 minutes a day for 2 consecutive days, with Froot Loop pieces (Kellogg's Company, Battle Creek, MI) scattered throughout the maze to encourage exploration. Following habituation, once rats were comfortable on the testing apparatus, they were trained to alternate between the left and right turns for 32 trials per day or 30 min. Every day a rat began testing by being placed on the continuous-T maze at the location labeled 'start' in Figure 1a. This proceeded for 1 week, then rats underwent the first baseline fMRI scan. For all behavioral testing sessions prior to the *Arc* experiment, rats completed 32 trials per day. Thus, performance and functional connectome differences could not be accounted for by a disparity in the number of trials completed between age groups.

After the baseline scan, rats began testing on the working memory/bi-conditional association task of cognitive multi-tasking (WM/BAT; Figure 1a). Each day, testing began by placing rats at the start location facing away from the choice platforms. After traversing the central arm, rats were initially allowed to run in whichever direction they chose, but on subsequent trials were only able to perform an object discrimination on a choice platform for reward if they alternated between trials. After making a correct turn, before returning to the center section of the maze, rats were 'interrupted' with an object discrimination problem on the choice platform in which a target object could be displaced and the animal received a Froot Loop piece. While the same object pair was presented in both the left and right choice

platforms, different objects are rewarded on the left versus right platform (owl was correct on the left platform and dog was correct on the right platform). Thus, animals had to integrate information about where in the maze they are with the object information to learn the correct bi-conditional association between an object and a place. Within a choice platform the location of the target object over the left or right food well varied pseudorandomly across trials. A single trail was considered leaving the start location, making a turn, then selecting an object, and returning to the start to begin the next trial. If a rat failed to alternate correctly, objects were not placed on the choice platform, no reward was available, this was recorded as a working memory error (WME), and not logged as a trial. The number of WMEs per day were recorded, but the percent correct was determined from the choice of the object. During WM/BAT training, rats performed 32 trials of object discrimination testing in each training session. On the first day of testing, objects were only partially covering the food reward for the first four trails per object (8 trials total) to encourage learning. Rats could begin with a trial turning in either the left or right direction, but on all subsequent trials, rats had to alternate turning directions. In addition to percent correct and WMEs, a response bias was calculated for each day of testing. This metric captures an animal's tendency to select an object over a food well on a particular side, regardless of object identity. The response bias was calculated for each testing session as the absolute value of the difference between choosing the object over the left well versus the right well divided by the total number of trials. Thus, 1 indicates a maximal bias in which only one side was selected and 0 is representative of no bias. Because the target object was presented over the left versus right food wells for an equal number of trials, object placement did not influence the response bias, and if a rat performed perfectly the response bias would be 0. Rats were tested on the WM/BAT for eleven consecutive days and then given 2 days off during which the second scanning session occurred. After the scans were completed, rats tested for another 14 days and were scanned for a third and final time. After the last scan, rats were retrained on the WM/BAT with a new set of objects for the *Arc* catFISH experiment.

In the second group of rats, animals were food restricted and shaped to get familiar with the maze using the same procedures described above, and then were given a baseline resting state fMRI scan. After the baseline scan, these rats then traversed the maze for a froot loop reward for 32 traversals/day and were scanned after 11 and 24 days of maze running. The rats in this experiment served as a control group that did not undergo cognitive training.

Functional magnetic resonance imaging. Rats were imaged under isoflurane (1.5%) sedation (delivered in 70%N_2/30%O_2 at 0.1L/min). Inhalation anesthetics (e.g., isoflurane) are preferred for longitudinal fMRI experiments over intravenous injectable anesthetics due to better control over blood levels of the sedative, fast recovery and lower mortality rates in rats. Important to the present study, several studies have confirmed BOLD activation patterns at low levels of anesthesia in rats (Masamoto et al., 2007; Kannurpatti et al., 2008; Kim et al., 2010; Williams et al., 2010). Isoflurane induces dose-dependent vasodilation; thus, functional experiments must be ideally performed under doses lower than 2% (i.e., a fixed concentration between 1 and 1.5%) as was done in the current study (fixed at 1.5%). Even in human neuroimaging studies, general anesthesia (sevoflurane) has been shown to not prevent the measurement of BOLD activity and general connectivity (Riehl et al., 2018). Spontaneous breathing was monitored during MRI acquisition (SA Instruments, Stony Brook, NY). Body temperature was maintained at 37-38°C using a warm water recirculation system. Heads were stabilized using a bite bar and foam side padding and the surface coil was placed over the rats' head (providing further restrictions to movement). The motion correction is implemented as a default step since minor head movements is always possible, although our prior work and work in this study shows no evidence of any gross movement (e.g., Febo and Ferris, 2014; Colon-Perez et al., 2016b; Orsini et al., 2018).

In the group of rats that received cognitive training, a resting state fMRI dataset was collected in an 11.1 Tesla Bruker system (Magnex Scientific). The system is a Bruker AV3 HD console/Paravision 6.01 with a volume transmit (85mm inner diameter quadrature coil), and a 4-

channel phase-array receive coil (Rapid Rat Phase Array). All ten rats were scanned over the span of two months in three scanning sessions: before cognitive training (baseline scan; n_{young} = 5, n_{old} = 5), following 11 days of training (scan 2), and after an additional two weeks of training (scan 3). A 1-shot spin echo EPI sequence was acquired with acquisition parameters: TR/TE = 2000/15 ms, and 300 repetitions for a total acquisition time of 10 mins (an image was acquired every 2s), FOV = 25.6 x 25.6 mm^2, 20 slices 1 mm thick, and data matrix = 64 x 64. The voxel size was 0.4 mm in place, which is within range of geometric parameters of most rat fMRI studies. Anatomical scans for image overlay and reference-to-atlas registration were collected using a fast spin echo sequence, with the following parameters: TR/TE_{eff} = 4500/48 ms, RARE factor = 16, and number of averages = 6, FOV = 25.6 x 25.6 mm^2, 20 slices 1.0mm thick, and data matrix = 256 x 256.

Due to technical issues with the 4-channel phase-array receive coil that emerged after the completion of the cognitive training experiment, resting state fMRI scans for the rats that did not receive cognitive training were collected on a 4.7 T/33 cm horizontal magnet (Magnex Scientific) with an 11.5-cm-diameter gradient insert (670 mT/m maximum gradient strength at 300 A and a 120 µs rise time; Resonance Research) and controlled by VnmrJ 3.1 software (Agilent). A quadrature transmit/receive radio frequency (RF) coil tuned to 200.6 MHz 1H resonance was used for B1 field excitation and RF signal detection (Air MRI). Functional images were collected using a two-shot spin-echo echoplanar imaging (EPI) sequence with the following parameters: echo time (TE) = 50 ms; repetition time (TR) = 1 s; 32.5 × 32.5 mm in plane (voxel size = 0.5 mm); 12 slices with 1.5 mm thickness per slice; data matrix = 64 × 64. A total of 300 repetitions were collected per EPI scan (10 min), with two scans per rat. Anatomic scans for image overlay and reference-to-atlas registration were collected using a fast spin echo sequence (TE = 45 ms; TR = 2 s; echo train length = 8; number of averages = 10; data matrix = 256 × 256) in the same space as the EPI scan.

Image processing. Image processing and network calculations from functional connectivity-based graphs were as previously implemented and reported for mouse (Colon-Perez et al., 2019), rat (Orsini et al., 2018), and Marmoset monkey brains (LaClair et al., 2019). Brain masks were drawn manually over high-resolution anatomical scans using segmentation tools in itkSNAP (www.itksnap.org). The masks were used to crop images and remove non-brain voxels. The cropped brain images were aligned with a rat brain template using the FMRIB Software Library linear registration program *flirt* (Jenkinson et al., 2002), using previously published parameters (Colon-Perez et al., 2016a). Registration matrices were saved and used to subsequently transform functional datasets into atlas space for preprocessing and analysis. Slight displacements in individual images over the series of 300 images and slice timing delays were corrected, and time series spikes were removed using Analysis of Functional NeuroImages (AFNI)(Cox, 1996). Linear and quadratic detrending, spatial blurring, and intensity normalization were also performed. Six head motion parameters and cerebroventricular and white matter signals were removed from all datasets. A voxelwise temporal band-pass filter (between 0.01 Hz and 0.1 Hz) was applied to remove brain signals that contain cardiac and respiratory frequencies.

Time series fMRI signals were extracted from each region of interest (ROI) based on the atlas-guided seed location (150 total areas, divided equally in left and right representations of each region). This is a segmentation atlas based on the Paxinos and Watson atlas of the rat brain (Paxinos and Watson, 1998). It was developed by Ekam imaging (Northeastern University, Boston) (Yee et al., 2015), and has been used in a number of previous publications (e.g., Febo et al., 2009; Nephew et al., 2009; Colon-Perez et al., 2018; Nephew et al., 2018). Signals were averaged from voxels in each ROI (Colon-Perez et al., 2016a). Voxel-wise cross-correlations were carried out to create correlation coefficient (Pearson r) maps. The first 9 images in each functional time series were not used in the cross-correlation step. Pearson r maps were subjected to a voxelwise z-transformation. AFNI's *3dClustSim* program was used to determine

the adequate cluster size for a given uncorrected *p*-value. The resultant voxel cluster size at p ≤ 0.05 was used to control the level of false positive rates in the final composite statistical maps.

Network analysis. Brain connectivity networks were analyzed using the Brain Connectivity Toolbox for Matlab (Rubinov and Sporns, 2010) and as previously reported (Colon-Perez et al., 2018; Orsini et al., 2018). Symmetrical connectivity graphs with a total 11,175 matrix entries were first organized in Matlab [graph size = n(n-1)/2, where n is the number of nodes represented in the graph of 150 ROI]. The z score values of the graphs were thresholded for each subject to create matrices with equal densities (e.g., z values in the top 15% of all possible correlation coefficients). Matrix z values were normalized by the highest z-score, such that all matrices had edge weight values ranging from 0 to 1. *Node strength* (sum of edge weights), *clustering coefficient* (the degree to which nodes cluster together in groups), *average shortest path length* (the potential for communication between pairs of structures), and *small-worldness* (the degree to which rat functional brain networks under study deviate from randomly connected networks) were calculated for these weighted graphs (Newman, 2003; Boccaletti et al., 2006; Saramaki et al., 2007). Brain networks were visualized using BrainNet (Xia et al., 2013). The 3D networks were generated with undirected edges weights $E_{undir} \geq 0.3$. In these brain networks (or rat brain connectomes), the node size and color was scaled by the node strength and edges were scaled by z-scores. Subnetworks with high node strength (after retaining ≥15% top graph density per subject) were further analyzed to examine for potential effects of cognitive training. This was based on the qualitative observation that in the aged rats, the representation of nodes with high strength and high degree changed between the baseline and subsequent scans. Critically, the experimenters that conducted the connectivity analyses were completely blind to behavioral variables. Finally, as an unbiased measure of network organization, the *rich club* coefficient was calculated as the number of edges that connect nodes with degree k or higher. This measures the extent to which high-edge nodes are more likely to be connected to each other.

Tissue collection and Arc catFISH. To investigate potential age-related differences in neuron activity during WM/BAT performance, we trained young and aged rats on a new problem set for 13 days. On the 14th day of testing, rats performed both the WM/BAT and a control spatial alternation task in which a food reward was randomly placed in a food well on the choice platform. The reward was not covered by an object and rats did not have to perform the discrimination problem in this control task. After this first epoch of behavior, rats were placed in their home cages for a 20-min rest. Following the rest, rats performed a second epoch of behavior for 5 min. All rats performed one epoch of WM/BAT and one epoch of spatial alternation in counterbalanced order. Immediately following the second epoch of behavior, rats were placed into a bell jar containing isoflurane-saturated cotton (Abbott Laboratories, Chicago, IL, USA), separated from the animal by a wire mesh shield. Animals lost righting reflex within 30 seconds of being placed within the jar and immediately euthanized by rapid decapitation. Tissue was extracted and flash frozen in 2-methyl butane (Acros Organics, NJ, USA) chilled in a bath of dry ice with 100% ethanol (~-70ºC). One additional rat in each age group was sacrificed directly from the home cage as a negative control during the experiment to ensure that disruptions within the colony room do not lead to robust nonexperimental behaviorally-induced *Arc* expression. Tissue was stored at -80ºC until cryosectioning and processing for fluorescence in situ hybridization to label the mRNA products of the immediate-early gene *Arc* for cellular compartment analysis of temporal activity with fluorescence *in situ* hybridization (catFISH).

Tissue was sliced at 20-µm thickness on a cryostat (Microm HM550) and thaw-mounted on Superfrost Plus slides (Fisher Scientific). Fluorescence *in situ* hybridization (FISH) for the immediate-early gene *Arc* was performed as previously described (Guzowski et al., 1999). Briefly, a commercial transcription kit and RNA labeling mix (Ambion REF #: 11277073910, Lot #: 10030660; Austin, TX) were used to generate a digoxigenin-labeled riboprobe using a plasmid template containing a 3.0 kb Arc cDNA (Steward et al., 1998). Tissue was incubated

with the probe overnight, and *Arc*-positive cells were detected with antiedigoxigenin-HRP conjugate (Roche Applied Science Ref #: 11207733910, Lot #: 10520200; Penzberg, Germany). Cy3 (Cy3 Direct FISH; PerkinElmer Life Sciences, Waltham, MA) was used to visualize labeled cells, and nuclei were counterstained with DAPI (Thermo Scientific). The subcellular localization of *Arc* mRNA can be used to determine which neuronal ensembles across the brain were active during 2 distinct episodes of behavior. *Arc* is first transcribed within the nucleus of neurons 1-2 minutes after cell firing. Importantly, *Arc* mRNA translocate to the cytoplasm approximately 15-20 minutes after cell firing, which allows for cellular activity during 2 epochs of behavior, separated by a 20-min rest to be represented within a single neural population (Guzowski et al., 1999).

Z-stack images were collected by fluorescence microscopy (Keyence; Osaka, Osaka Prefecture, Japan) in increments of 1 µm. Four images (2 from superficial layers and 2 from deep layers; Figure 6a) were taken from the anterior cingulate cortex (ACC) of both the left and right hemispheres from 3 different tissue sections for a total of 24 images for each rat. Six images (3 from medial and 3 from lateral) were taken from both hemispheres of the dorsal striatum (DS) for a total of 36 images per rat. The percentage and subcellular location of Arc-positive cells was determined by experimenters blind to age and order of behavioral tasks using ImageJ software with a custom written plugin for identifying and classifying cells. Nuclei that were not cutoff by the edges of the tissue and only those cells that were visible within the median 20% of the optical planes were included for counting. All nuclei were identified with the *Arc* channel off, as to not bias the counter. When the total number of cells in the z-stack were identified, the *Arc* channel was turned on to classify cells as positive for nuclear *Arc*, cytoplasmic *Arc*, both nuclear and cytoplasmic *Arc*, or negative for *Arc*. A cell was counted as *Arc* nuclear positive if 1 or 2 fluorescently labeled foci could be detected above threshold anywhere within the nucleus on at least 4 consecutive planes. A cell was counted as *Arc* cytoplasmic positive if fluorescent labeling could be detected above background surrounding at

least 1/3 of the nucleus on 2 adjacent planes. Cells meeting both of these criteria were counted as *Arc* nuclear and cytoplasmic positive.

Neural activation during the WM/BAT and spatial alternation tasks was examined using the percentage of cells positive for cytoplasmic and/or nuclear Arc expression. A mean percentage of cells was calculated for each rat for each brain region and condition, so that all statistics were based on the number of animals for sample size, rather than images or cells. This avoids the caveat of inflating statistical power and having different dependent variables correlate with each other, which can be the case in nested experimental designs (Aarts et al., 2014). Critically, the order of behavior was counterbalanced across rats, with equal numbers in both age groups, such that cytoplasmic staining corresponded to WM/BAT task behavior and nuclear staining corresponded with alternation behavior for half of the rats and vice versa for the others. Thus, all plots showing mean percentage of *Arc*-positive cells are in reference to the task and not the epoch. Notably, as in other previous studies with similar behaviors (Hernandez et al., 2018b), task order did not have a significant impact on neuron activity levels.

Potential effects of age and brain region on the percentage of cells expressing *Arc* during the different behaviors (WM/BAT versus spatial alternation) were examined with factorial ANOVAs. All analyses were performed using Statistical Package for the Social Sciences (SPSS), v.25 or v.26, software. Statistical significance was considered at p values less than 0.05.

RESULTS

Working memory/biconditional association task (WM/BAT) performance. Rats can make two different types of errors on the WM/BAT. They can select the incorrect object, as well as take the same turn direction on adjacent trials. The latter is considered a working memory error (WME). Previous studies have reported that the primary type of error made by rats is selecting the incorrect object, and that there is not a significant effect of age group on the number of WMEs (Hernandez et al., 2015; Hernandez et al., 2018b). Figure 1b-d summarizes the mean

417 percent correct for selecting the target object for young (black) and aged (grey) rats across
418 testing days for the first (Figure 1b) and the second (Figure 1d) WM/BAT problem sets.
419 Between the first and second scan, there was not a significant main effect of testing day ($F_{[10,80]}$
420 = 0.74, p = 0.68), age ($F_{[1,8]}$ = 1.71, p = 0.27), or an age by test day interaction ($F_{[10,80]}$ = 0.45, p
421 = 0.92). In contrast, between the second and third scan, there was a significant main effect of
422 testing day ($F_{[13,91]}$ = 3.84, p = 0.019). Orthogonal contrasts comparing each day of testing to
423 performance on the day following the second scan (Day 12) indicated that the percentages of
424 correct responses were significantly greater by day 17 compared to day 12 (p = 0.038). There
425 was also a trend for an age effect ($F_{[1,8]}$ = 4.30, p = 0.07), but no significant interaction between
426 age and test day ($F_{[13,91]}$ = 1.09, p = 0.38). Another way to evaluate the performances of young
427 and aged rats is to compare the total number of incorrect trials during training. Across all days
428 of testing, the aged rats made significantly more errors than the young rats ($F_{[1,8]}$ = 10.02, p =
429 0.013). Importantly, there was a significant interaction effect between age and phase of testing
430 (Days 1-11 versus Days 12-25; $F_{[1,8]}$ = 5.54, p = 0.046). Post hoc analysis indicated that young
431 and aged rats made a similar number of errors prior to the second scan (Days 1-11; $T_{[8]}$ = 0.55,
432 p = 0.60), but aged rats made significantly more errors prior to the third scan (Days 12-25; $T_{[8]}$ =
433 3.50, p = 0.008, corrected α = 0.025). After the third scan, rats were retrained on WM/BAT with
434 different objects for 13 days before performing the task a final time, followed by immediate
435 sacrifice to label the mRNA products of the activity-dependent immediate-early gene *Arc*
436 (Guzowski et al., 1999). Overall, rats showed significant improvements across days of testing
437 for selecting the correct object ($F_{[13,91]}$ = 2.91, p = 0.01). Moreover, the interaction effect
438 between age and test day was statistically significant ($F_{[13,91]}$ = 2.14, p = 0.02), with aged rats
439 performing similar to young on the first two test days, but significantly worse on the final day
440 ($F_{[1,7]}$ = 5.29, p = 0.05). Thus, across two different WM/BAT problems sets aged rats performed
441 worse than young animals.
442 Consistent with previous data, there was not a significant effect of age group on the

number WMEs (Hernandez et al., 2015). Figure 1d shows the mean number of WMEs per day during the testing sessions between resting state scans and for the *Arc* experiment. Although the rate of WMEs did not vary by age group ($F_{[1,8]} = 0.24$, $p = 0.64$), it did significantly decrease across testing ($F_{[2,16]} = 14.31$, $p = 0.001$). Importantly, the rate of WMEs across testing session did not significantly interact with age group ($F_{[1,16]} = 0.44$, $p = 0.65$), suggesting that this type of performance error could not account for the different effects of cognitive training on the functional connectome between young and old rats.

Previous studies have reported that before animals learn an object discrimination problem, they show a significant response bias by selecting an object over a food well on a particular side (left versus right) regardless of object identity (Lee and Byeon, 2014; Hernandez et al., 2015; Johnson et al., 2017a). This innate response bias must be overcome before animals will learn the biconditional rule (Lee and Byeon, 2014). Figure 2a shows the mean response biases for young and aged rats across testing sessions between resting state scans. The response bias did not significantly change across testing days 1-11 ($F_{[10,80]} = 0.81$, $p = 0.62$), and there was not a significant difference in the response bias between young and aged rats between scans 1 and 2 ($F_{[1,8]} = 0.81$, $p = 0.19$). Prior to scan 2, the interaction effect of age and testing day also did not reach statistical significance ($F_{[10,80]} = 0.88$, $p = 0.56$). Between scans 2 and 3, across testing days 12-25, the response bias also did not significantly change as a function of test day ($F_{[13,104]} = 1.03$, $p = 0.43$), and there was not a significant effect of age ($F_{[1,8]} = 2.92$, $p = 0.13$). The interaction effect between testing day and age, however, did reach statistical significance ($F_{[13,104]} = 2.70$, $p < 0.01$). This was due to the young and aged rats having a similar response bias across days 12-17, but the young rats having a decreasing bias on the later testing days. This decreasing bias as a function of testing was not observed in aged rats. Figure 2b shows the mean response bias for young and aged rats while being trained on the new WM/BAT problem for the *Arc* experiment. In this phase of cognitive training, the response bias did not change as a function of testing day ($F_{[13,91]} = 1.23$, $p = 0.27$). Although the

interaction effect of age and test day was also not significant ($F_{[13,91]} = 0.99$, $p = 0.47$), the aged rats overall had a significantly higher response bias relative to young animals ($F_{[1,7]} = 6.41$, $p = 0.04$). To further examine how the response bias might relate to experimental stage, the biases on days adjacent to resting state scans and during the *Arc* experiment were also examined. Figure 2c shows the mean response biases on the first day of testing after the baseline scan, on the days before scans 2 and 3, and on the day of the *Arc* experiment for young and aged rats. Across these critical experimental days, there was not an overall significant effect of day on the response bias ($F_{[3,21]} = 0.51$, $p = 0.68$), but aged rats had a significantly larger response bias relative to the young animals ($F_{[1,7]} = 49.83$, $p = 0.0001$), consistent with previous reports (Hernandez et al., 2015; Johnson et al., 2017a). The interaction effect between age and day was also significant ($F_{[3,21]} = 10.60$, $p = 0.014$). Post hoc analyses indicated that young and aged rats showed comparable response biases on the first day of testing ($T_{[8]} = 0.25$, $p = 0.81$), a trend towards an age effect prior to scan 2 ($T_{[8]} = 1.88$, $p = 0.09$), and a significantly higher response bias in aged relative to young rats prior to scan 3 ($T_{[8]} = 4.66$, $p = 0.002$, corrected $\alpha = 0.05/4 = 0.0125$) and during the *Arc* experiment ($T_{[7]} = 3.35$, $p = 0.012$, corrected $\alpha = 0.05/4 = 0.0125$). These data suggest that all rats began testing with a response bias, but the young animals abandoned this suboptimal strategy early in training. In contrast, the aged rats perseverated and continued to use this strategy across testing sessions.

The effect of cognitive training on resting state connectivity. Over the past decade, graph theoretical approaches have been widely used to quantify functional brain networks (Bullmore and Sporns, 2009, 2012; Ash and Rapp, 2014). This analytical approach models the brain as a complex network composed of nodes (that is, brain regions) and edges (that is, functional correlations) connecting the nodes (Bullmore and Sporns, 2009). Figure 3a/b shows the 3D brain networks with functional edges with z-scores larger than 0.3 in young and aged rats across scanning sessions. Quantified metrics for global network connectivity included node strength, node degree, path length and clustering coefficient, which are defined in Table 1.

None of these variables were significantly affected by scanning session, age, nor did the scanning session by age interaction reach significance (see Table 2 for statistical summary). These findings are consistent with a previous study reporting that resting state networks are consistent over time (Iordan et al., 2017).

Table 2: Quantification of global inter-node connectivity patterns

Variable	Scanning Session	Age	Scanning Session x Age Interaction
Node strength	$F_{[2,29]} = 1.06$, $p = 0.36$	$F_{[1,29]} = 0.52$, $p = 0.47$	$F_{[2,29]} = 0.21$, $p = 0.81$
Node degree	$F_{[2,29]} = 0.50$, $p = 0.61$	$F_{[1,29]} = 2.00$, $p = 0.17$	$F_{[2,29]} = 0.50$, $p = 0.61$
Path length	$F_{[2,29]} = 0.86$, $p = 0.44$	$F_{[1,29]} = 0.59$, $p = 0.45$	$F_{[2,29]} = 0.10$, $p = 0.90$
Clustering coefficient	$F_{[2,29]} = 0.54$, $p = 0.59$	$F_{[1,29]} = 0.11$, $p = 0.73$	$F_{[2,29]} = 0.41$, $p = 0.67$

Figure 3c/d shows the distributions of node strength and node degree, respectively, for the young and aged rats. It is qualitatively evident from these distributions that in the aged rats there was a change across scanning sessions in patterns of connectivity that reflected an increased representation of nodes with high strengths ($s > 15$; Figure 3c) and high degree (degree (k) > 40; Figure 3d) between the baseline and subsequent scan sessions (blue arrows; Figure 3c/d). From this distribution, 16 nodes with strength values larger than 15 during the second scan session in the aged rats were identified. Figure 4 shows the connectivity between these nodes in young (Figure 4a) and aged (Figure 4b) rats across scanning session, as well as the associated brain regions for these 16 nodes (Figure 4c). The anterior cingulate cortex (ACC) was identified as a node with higher strength values as a function of WM/BAT training in both hemispheres. Because there are known age-related physiological changes within this region (Insel et al., 2012; Insel and Barnes, 2015), and morphological differences in this structure are implicated in successful aging (Rogalski et al., 2012), we used the ACC as a seed to quantify functional connectivity between this region and other nodes in relation to scan session (Figure 5a). This analysis revealed that the functional connectivity between ACC and dorsal striatum (DS) in the both the lateral (DSL) and medial (DMS) subregions changed as a function of scan

session and age (Figure 5b). Although ACC-DLS and ACC-DMS connectivity was measured separately for each hemisphere, there was no significant main effect of left versus right hemisphere ($F_{[1,32]} = 0.001$; $p = 0.97$) and these were averaged together. The main effect of scan session on ACC-DS connectivity did not reach statistical significance ($F_{[2,64]} = 1.69$; $p = 0.19$). Moreover, the strength of the connectivity between the ACC and DLS versus DMS was not significantly different ($F_{[1,32]} = 1.15$; $p = 0.29$). There was, however, a trend for aged rats to have significantly higher ACC-DS connectivity compared to young animals ($F_{[1,32]} = 3.67$; $p = 0.07$). Importantly, the interaction between age and scan session was significant ($F_{[2,64]} = 3.75$; $p = 0.03$). Post hoc analysis indicated that there were no significant age differences between ACC-DS connectivity during the baseline scan (95% confidence interval: -0.11 to 0.17, $p = 0.63$), and scan 2 (95% confidence interval: -0.24 to 0.07, $p = 0.26$), but the aged rats had significantly higher connectivity relative to young during the third scan (95% confidence interval: -0.42 to -0.09, $p = 0.004$). These data are interesting in the context of the behavioral results showing that aged rats have a significantly larger response bias across training relative to the young (Figure 2). It is well established that the DS is involved in response-based learning strategies (Packard and McGaugh, 1992; Gold, 2004), and aged rats may default to more response-based strategies as spatial learning becomes impaired (Barnes et al., 1980; Tomas Pereira et al., 2015). Thus, the increased ACC-DS connectivity observed here may be a network signature of the enhanced response bias seen at the behavioral level.

To further examine the idea that enhanced ACC-DS connectivity was related to the higher response bias in aged rats with poor performance, we quantified the correlation between ACC-DS connectivity and the response bias across the 3 scanning sessions. To avoid detecting a spurious correlation due to age differences, all variables were transformed to z-scores calculated for the different age groups separately. This approach accounts for the tendency to detect spurious correlations due to age differences rather than an actual relationship between variables (Gerrard et al., 2008). Figure 6 shows the response bias at three

543 different time points across training measured during days adjacent to the scanning session
544 plotted as a function of ACC-DS connectivity. Across the 3 scanning sessions ACC-DS
545 connectivity accounted for a significant amount variance in the normalized mean response bias
546 of individual rats ($R_{[27]} = 0.48$, $F_{[1,27]} = 8.19$, $p = 0.008$), such that more connectivity
547 corresponded with a higher proportion of trials in which this aberrant strategy was used. Note
548 that the correlations were similar when both aged groups were considered separately ($R = 0.47$
549 for young and $R = 0.49$ for aged), and when age was entered as a covariate into the model it did
550 not account for a significant amount of the variance in the relationship between normalized
551 ACC-DS connectivity and normalized response bias ($R = 0.01$, $p = 0.95$). This observation
552 suggests that in the young animals, the decreasing response bias across cognitive testing may
553 have been facilitated by a concurrent decrease in ACC-DS connectivity. In contrast, the abilities
554 of aged rats to inhibit a response-based strategy may have been hindered by ACC-DS
555 connectivity that increased across testing.
556 Because of the potential presence of a subnetwork of 'hub' nodes driving the network
557 patterns in older rats, we next assessed the "rich club" index. Rich club indices were calculated
558 for young and aged rats as a function of scanning session. Figure 7 shows the rich club
559 organization in young and aged rats at baseline (Figure 7a) and after cognitive training (Figures
560 7 b/c) as a function of edge degree (k). Similar to previous reports from human study
561 participants (Cao et al., 2014a), the functional rich club architecture during the baseline scan
562 was significantly reduced in aged rats relative to young for rich club indices quantified at high
563 edge degrees (k-level > 27, $p < 0.05$). The young rats had stable functional rich club
564 organization across all scans (Figure 7b), which has previously been reported (Liang et al.,
565 2018). Interestingly, in the aged rats there was a significant increase in rich club participation
566 after the baseline scan (Figure 7c). Starting after the first training period (11 days), rich club for
567 indices for edge values larger than 20 displayed a significant main effect of scanning session
568 ($F_{[2,29]} > 3.4$, $p < 0.05$, for all comparisons), but not of age ($F_{[1,29]} < 0.55$, $p > 0.5$, for all

569 comparisons). The interaction effect of age and scanning session, however, was statistically
570 significant for large k levels (k > 28) ($F_{[2,29]} > 3.80$, $p < 0.05$, for all comparisons). As evident in
571 Figures 7b/c, the significant interaction between scan session and rich club participation was
572 due to the aged rats having greater rich club indices after cognitive training, while the young rats
573 did not show a change.

574 *Behaviorally-induced expression of the immediate-early gene Arc.* Due to the elevated
575 response bias of aged rats (Figure 2b/c), and the observation that the old animals showed an
576 increase in ACC-DS connectivity as a function of cognitive training, we focused our *Arc* catFISH
577 analysis on the ACC and DS. Figure 8a shows the region of ACC that was imaged and
578 representative examples of *Arc* labeling in a young and an aged rat. The percentage of ACC
579 neurons activation during the WM/BAT and spatial alternation task are shown for young and
580 aged rats in Figure 8b. Repeated-measures ANOVA with the within subject factor of task and
581 the between subjects factors of age group, hemisphere and cortical layer did not detect a
582 significant difference in the proportion of cells activated during WM/BAT versus spatial
583 alternation ($F_{[1,28]} = 1.53$, $p = 0.23$). Additionally, none of the other between subjects factors
584 reached statistical significance ($F_{[2,28]} < 3.01$, $p > 0.09$, for all comparisons), nor were any of the
585 interaction terms significant ($F_{[1,28]} < 2.99$, $p > 0.1$, for all comparisons).

586 Figure 8c shows the areas of the DS that images were collected from, as well as
587 representative examples of *Arc* labeling in young and aged rats. To match the functional
588 connectivity analyses, samples were taken from both the medial and lateral DS. Figure 8d
589 shows the percentages of DS neurons that were positive for *Arc* during the different tasks in
590 young and aged rats. Repeated-measures ANOVA with the within subject factor of task and the
591 between subjects factors of age group, hemisphere and subregion (medial versus lateral DS)
592 indicated that there was not a significant main effect of task on the percentage of cells positive
593 for *Arc* ($F_{[1,28]} = 1.24$, $p = 0.28$). The aged rats, however, had significantly more cells that were
594 positive for *Arc* compared to the young animals ($F_{[1,28]} = 5.58$, $p < 0.03$). This age difference

595 was observed in both the medial and lateral DS, as indicated by lack of a main effect of
596 subregion ($F_{[1,28]} = 0.85$, $p = 0.37$). The interaction effect between age and task was also
597 significant ($F_{[1,28]} = 13.64$, $p < 0.001$), such that aged rats had more cells than young rats that
598 transcribed *Arc* during WM/BAT ($p < 0.001$), but this same difference was not observed during
599 the alternation task ($p = 0.43$). These data indicate that the enhanced DS activation in aged
600 rats was specific to the behavioral in task in which the old animals demonstrated a deleterious
601 response bias associated with worse performance. No other interaction effects reached
602 statistical significance ($F_{[1,28]} < 1.81$, $p > 0.18$, for all comparisons). Due to the relatively small
603 numbers of animals that both received longitudinal resting state fMRI scans and were examined
604 for *Arc* expression, we also measured WM/BAT-related *Arc* expression in the DS for a second
605 group of rats (n = 7 young and n = 8 aged). These rats were tested over 2 weeks and then
606 sacrificed directly following behavior using identical procedures to the first cohort. As with the
607 first cohort, the aged rats performed significantly worse than the young ($T_{[14]} = 3.21$, $p = 0.006$),
608 and had a significantly higher response bias ($T_{[14]} = 2.64$, $p = 0.01$). Moreover, the average
609 percent of *Arc* positive cells in the DS was 3.56% for the aged rats and 2.01% for the young.
610 This was comparable to the levels of *Arc* expression observed for the first cohort. Moreover, in
611 this second cohort of animals, the aged rats had significantly more cells in the DS that were *Arc*
612 positive compared to the young animals ($T_{[14]} = 2.22$, $p = 0.04$). Notably, the response bias
613 index in 6 of the 8 aged rats was >0.9 (near ceiling), which did not allow for sufficient parametric
614 space to detect potential correlations. However, the two aged rats with lower response bias
615 indices (0.06 and 0.25) also had levels of *Arc* positive cells that were in the range of young
616 animals (1.63% and 1.93%, respectively). These data confirm our initial observations and
617 further support the idea that elevated activity the DS is related to suboptimal response-based
618 behavior during WM/BAT testing.

619 It is conceivable that behavioral differences other than the elevated response bias could
620 account for the increased *Arc* in the DS of aged rats, such as differences in the number of trials

completed or rewards received. The number of trials completed during the *Arc* experiment was compared across tasks and aged groups with repeated-measures ANOVA with the within-subject factor of task and the between-subjects factor of age group. This comparison did not detect a significant difference in the number of WM/BAT and spatial alternation trials completed ($F_{[1,7]} = 2.31$, $p = 0.17$). Moreover, the main effect of age did not reach statistical significance ($F_{[1,7]} = 3.31$, $p = 0.11$), nor was the interaction between age and task significant ($F_{[1,7]} = 0.61$, $p = 0.46$). Thus, the differences in neuron activation in DS could not be explained by animals performing a different number of trials.

Another possibility for the elevated *Arc* expression in the DS of aged compared to young rats could be due to reward expectancy error from the aged rats receiving fewer rewards during WM/BAT testing compared to the young animals. Figure 9a shows the mean number of rewards received for the young and aged rats across the WM/BAT and control alternation task. Rats received more rewards during the alternation task compared to WM/BAT ($F_{[1,7]} = 27.27$, $p = 0.001$). There was also a trend for aged rats to receive fewer rewards than young ($F_{[1,7]} = 5.55$, $p = 0.051$), and for this to interact with task ($F_{[1,7]} = 3.67$, $p = 0.097$). If differences in reward experience across tasks were to account for altered expression patterns of *Arc* in the DS, then one could predict that the overlap in active ensembles across tasks would be reduced in response to differences in reward experience. To examine the extent that the active neuronal ensemble changed between the different tasks, a similarity score was calculated. As population overlap can be affected by differences in overall activity levels, similarity scores can be calculated to control for differences in activity between regions (Vazdarjanova and Guzowski, 2004). The similarity scores were compared between the ACC, DLS and DMS (within-subjects factor of region), and the between-subjects variable of age. Because of reports that neurons in the DMS is more responsive to reward contingency and expectancy than the DLS (Balleine and O'doherty, 2010; Gremel and Costa, 2013; Regier et al., 2015), these regions were considered separately. Figure 9b shows the average similarity scores for young and aged rats for the

different regions of interest. The main effect of region was not significant ($F_{[2,14]} = 0.58$, $p = 0.57$), indicating that the ACC, DLS and DMS updated activity patterns similarly in response to performing a different task within the same environment. There was also not a significant main effect of age on similarity score ($F_{[1,7]} = 2.83$, $p = 0.14$), nor did the interaction effect between region and age reach statistical significance ($F_{[1,7]} = 0.15$, $p = 0.86$). The comparable similarity scores between age groups suggests that differences in reward experience cannot fully account for the elevated *Arc* expression in the DS in aged compared to young rats.

Anterior cingulate cortex (ACC)-dorsal striatum (DS) connectivity and rich club organization are stable across weeks of maze traversals in the absence of cognitive training. To enhance the rigor of the experiment showing that cognitive training altered the functional connectome of aged rats, but not young, an additional group of young and aged rats that did not perform the WM/BAT were longitudinally scanned at similar time intervals to the original experimental group (baseline, at 11 days, and at 24 days). These rats were trained to traverse a track for food reward for 32 trials/day to match the procedural and physical demands of the rats that received cognitive training. Figure 10 shows the connectivity between the ACC and the DSL (left panel) and DSM (right panel) as a function of scan session for the young and aged rats. In contrast to the rats that were cognitively trained, there was no interaction between age and scan session on the ACC-DS connectivity. Specifically, ACC-DS connectivity in the lateral (left) and medial (right) subregions did not significantly vary across scan session ($F_{[2,88]} = 0.39$, $p = 0.68$) or age group ($F_{[1,44]} = 0.57$, $p = 0.46$). Moreover, the interaction of age and scan was not significant ($F_{[2,88]} = 0.82$, $p = 0.44$). Finally, there was no effect of DS subregion ($F_{[1,44]} = 1.95$, $p = 0.17$) and none of the other interaction terms were statistically different ($P>0.1$ for all comparisons). These data suggest that cognitive training on WM/BAT was the likely reason for enhanced ACC-DS connectivity in aged rats during scan 3. Rich club organization was also examined in these rats. Figure 11 shows the rich club index in young and aged rats as a function of K-level. These values were consistent across scan session in the untrained rats in

673 both age groups ($p > 0.1$ for all comparisons).

674 **DISCUSSION**

675 The current study used a multi-scale imaging approach, integrating resting state fMRI
676 data with single-cell imaging of neuron activity, to determine the global network changes and
677 cellular activity patterns in young and aged rats in relation to cognitive training. Critically, the
678 resting state data were acquired longitudinally as a function of training on a working memory/bi-
679 conditional association task (WM/BAT). Similar to a previous report, the aged rats were
680 impaired on the WM/BAT relative to the young animals (Hernandez et al., 2015). Additionally,
681 the aged rats showed an elevated response bias during testing such that they often selected an
682 object on one side of the choice platform, regardless of their location on the maze (left versus
683 right platform), or the object identity (Figure 2). This suboptimal response-based strategy in
684 aged rats has been reported in other behavioral experiments (Hernandez et al., 2015; Johnson
685 et al., 2017b). Importantly, the ability to inhibit this response-driven strategy is dependent on
686 the medial prefrontal cortex and is associated with performance improvements (Lee and Byeon,
687 2014).

688 Several novel findings were found in this study. First, in the aged rats there was a
689 subnetwork that showed an increase in node strength and degree between the first scan
690 session and the two sessions that occurred after cognitive training (Figures 3 and 4). This
691 increase in node strength and degree, occurred independent of any significant increases in
692 cognitive performance. The increased node strength and connectivity was evident in the
693 anterior cingulate cortex (ACC) in both hemispheres, which is a brain region vulnerable in old
694 age (Vaidya et al., 2007; Insel et al., 2012). Moreover, anatomical variations in ACC
695 morphology have been implicated in successful aging (Gefen et al., 2015). Interestingly, when
696 the ACC was used as a seed for further functional connectivity analyses, both the lateral and
697 medial subregions of the dorsal striatum were identified as regions that showed resting state
698 connectivity with the ACC that changed over WM/BAT testing differentially in young and old

699 animals. In aged rats, ACC-DS functional connectivity increased as a function of cognitive
700 training. In contrast, the young animals showed no significant change in ACC-DS functional
701 connectivity between the baseline and subsequent scans. Despite functional distinctions
702 between the lateral and medial subregions of the DS, with the former being more related to
703 habits and response-driven behaviors (Balleine and O'doherty, 2010; Gremel and Costa, 2013;
704 Burton et al., 2015; Regier et al., 2015), the enhanced ACC-DS connectivity after cognitive
705 training in aged rats was observed in both the subregions.

706 In the current study, as in other work (Hernandez et al., 2015), when rats performed
707 poorly on the WM/BAT they exhibited a response bias. When examined across all scanning
708 sessions in both young and aged rats, the larger response biases were significantly correlated
709 with enhanced ACC-DS connectivity (Figure 6). This observation suggests that lower ACC-DS
710 connectivity is associated with improved behavioral performance and the ability of young rats to
711 suppress a response bias and correctly perform the WM/BAT. In support of this notion, it has
712 been reported that *Arc* expression in the DS of young mice decreases between early and late
713 learning as mice adopt an optimal strategy (Pooters et al., 2017). Thus, the higher levels of *Arc*
714 expression in the aged DS could be related to enhanced connectivity with the ACC and to the
715 aged animals not switching from a response-based to an object-in-place strategy. Alternatively,
716 it is also conceivable that the elevated expression of *Arc* in the DS of aged rats during behavior
717 was related to altered reward experience. Young animals received more rewards than aged
718 rats during the WM/BAT, but not during the control alternation task (Figure 9a). Importantly, the
719 young and aged had similar overlap in the active neural ensembles across tasks, suggesting the
720 difference reward experiences across tasks and age groups is unlikely to fully account for
721 elevated *Arc* expression in aged rats during WM/BAT performance.

722 The ACC directly projects to the DS (Gabbott et al., 2005; Fillinger et al., 2018), and both
723 structures are also indirectly connected through the central medial nucleus of the thalamus
724 (Vertes et al., 2012). The increased ACC-DS connectivity with training in aged rats may reflect

impaired suppression of response-based strategies. This idea is consistent with multiple lines of evidence. First, it is widely reported that aged animals with hippocampal-dependent spatial memory impairments tend to over utilize response-based strategies (Barnes et al., 1980; Tomas Pereira et al., 2015), that are supported by the DS (Packard and McGaugh, 1992; Graybiel, 1998; Pych et al., 2005). Second, successful performance on the WM/BAT requires animals to flexibly update their behavior based on their position in the maze. Set-shifting is compromised in aged rats (Barense et al., 2002; Beas et al., 2013; Beas et al., 2016), and this deficit has been linked to age-associated neurobiological alterations in the ACC and DS (Nicolle and Baxter, 2003; Nieves-Martinez et al., 2012). Finally, it is striking that the aged rats with less flexible and more response-driven behavior had high cellular *Arc* activity levels in the DS during performance of the WM/BAT, but not during the control spatial alternation task. It is known that neurons in DS that express *Arc* are GABAergic principal cells that are also positive for CaMKII (Vazdarjanova et al., 2006). A previous study showed that stochastic spatial exploration induces ~5% of DS neurons to express *Arc* in young rats (Vazdarjanova et al., 2006). The current study adds to our understanding of *Arc* in DS by showing that when animals employ response-driven behaviors, as the aged rats did during WM/BAT performance, there is an increased engagement of DS neurons. Taken together these multi-scale imaging data therefore suggest that the DS may be overactive during cognitive training in association with response-driven behaviors. Enhanced DS activity during behavior could be related to a reduced ability of the ACC to inhibit the DS, which then manifests as enhanced ACC-DS resting state connectivity and perseverative suboptimal behavior.

An additional novel finding from the current data is the observation that rich club organization changed over cognitive training in aged, but not young, rats. The baseline rich club indices for nodes with high edge values ($k > 27$) was lower in aged compared to young rats (Figure 7a). This observation is consistent with data from human study participants that have reported less functional rich club participation in older compared to younger adults (Cao et al.,

2014a). As in previous studies (Liang et al., 2018), the young rats did not show a change in rich club participation across cognitive training (Figure 7b). In contrast, the aged rats had a significant increase in rich club participation between baseline and the second scan. This increase persisted in the third scan even though the aged rats displayed little to no improvements across the 25 days of cognitive testing (Figure 1b). These data are consistent with reports of network connectivity measures in humans, as a previous longitudinal study reported that older adults had less network stability over time compared to young study participants (Iordan et al., 2017). Moreover, enhanced rich club participation in aged rats could reflect a dedifferentiation of brain networks that has been observed in humans (Chan et al., 2014; Geerligs et al., 2014).

Rich club organization and the strength and proportion of long-distance connections are hypothesized to play a central role in optimizing global brain communication efficiency for normal cognition (Bullmore and Sporns, 2009, 2012; van den Heuvel et al., 2012). Presumably, at the foundation of the functional rich club are hub neurons that have long-rage projections. Interestingly, recent data have suggested that these neurons may be particularly vulnerable in advanced age with subsets of them being overrecruited during behavior in aged rats (Hernandez et al., 2018b). An over recruitment of vulnerable brain networks in aged animals during behavior could manifest as enhanced resting state rich club participation that ultimately reflect less adaptive networks and a reduced ability to recruit additional resources during behavior to improve performance. In line with this notion are recent data showing that higher levels of neural activity in prefrontal areas do not carry additional information related to cognitive performance (Morcom and Henson, 2018). In fact, elevated resting state connectivity could be related to reduced neural efficiency (e.g., Park et al., 2004; Nyberg et al., 2012) or a dedifferentiation in older networks (Carp et al., 2011; Hoffman and Morcom, 2018).

While the increases in connectivity and rich club participation observed in the current study could be consistent with age-related neural inefficiency, we cannot rule out the possibility

777 that activity differences in the aged rats are compensatory. While all old rats performed poorly at
778 WM/BAT relative to the young animals, aged and young rats were able to alternate similarly
779 showing comparable performance on the working memory component of the task. It is
780 conceivable that this aspect of the behavior was facilitated by the functional connectome
781 reorganization that occurred in the aged rats between the first and later scans. The aged rats,
782 however, were less able to recruit additional resources as cognitive load increase. This
783 interpretation of the data would be consistent with the Compensation-Related Utilization of
784 Neural Circuits hypothesis (CRUNCH). CRUNCH postulates that more neural resources are
785 recruited by older adults during tasks with minimal cognitive load. This increased activation,
786 could serve to compensate for a network that is compromised. As tasks become more difficult,
787 the limits of network capacity may be reached in older adults and these compensatory
788 mechanisms are no longer effective, leading to equivalent or less activation in older adults
789 relative to young (Reuter-Lorenz and Cappell, 2008; Grady, 2012). In the current experiments,
790 the older rats showed a quick increase in rich club participation even when they were unable to
791 correctly multi-task, suggesting that network limits in older rats are reached faster. In fact, these
792 data along with a recent cellular imaging study showing elevated *Arc* expression in the medial
793 prefrontal cortices of aged rats at rest (Hernandez et al., 2018b) indicate that baseline brain
794 connectivity of older animals may be close to maximum capacity with no cognitive load. If the
795 capacity of a network to respond to increasing cognitive load is constrained by increased rich
796 club participation, then aged rats may be less able to recruit additional resources when
797 cognitively multi-tasking. Ultimately, this elevated rich club participation in old animals could
798 contribute to the reduced dynamic range of neural activity that has been reported for older
799 adults (Kennedy et al., 2017).
800 An important impact of higher rich club participation and resting state connectivity in
801 aged rats could be to tax brain energy reserves that may already be compromised in advanced
802 age (Yoshizawa et al., 2014; Goyal et al., 2017; Hernandez et al., 2018a). Densely connected,

long distance projections are metabolically costly (Bullmore and Sporns, 2012). The higher costs associated with functional connections across multiple hubs makes them particularly vulnerable to metabolic deficiencies and cellular dysfunction contributing to instability in older animals. Thus, an enticing hypothesis is that improving the metabolic capacity of older animals could restore the dynamic range and functional rich club architecture. In the future, large-scale assessment of network connectivity in conjunction with single neuron activity dynamics and metabolic function could elucidate productive therapeutic avenues for treating cognitive aging.

References:

Aarts E, Verhage M, Veenvliet JV, Dolan CV, van der Sluis S (2014) A solution to dependency: using multilevel analysis to accommodate nested data. Nat Neurosci 17:491-496.

Ash JA, Rapp PR (2014) A quantitative neural network approach to understanding aging phenotypes. Ageing research reviews 15:44-50.

Ash JA, Lu H, Taxier LR, Long JM, Yang Y, Stein EA, Rapp PR (2016) Functional connectivity with the retrosplenial cortex predicts cognitive aging in rats. Proc Natl Acad Sci U S A 113:12286-12291.

Balleine BW, O'doherty JP (2010) Human and rodent homologies in action control: corticostriatal determinants of goal-directed and habitual action. Neuropsychopharmacology 35:48.

Barense MD, Fox MT, Baxter MG (2002) Aged rats are impaired on an attentional set-shifting task sensitive to medial frontal cortex damage in young rats. Learn Mem 9:191-201.

Barnes CA, Nadel L, Honig WK (1980) Spatial memory deficit in senescent rats. Can J Psychol 34:29-39.

Beas BS, Setlow B, Bizon JL (2013) Distinct manifestations of executive dysfunction in aged rats. Neurobiol Aging 34:2164-2174.

Beas BS, McQuail JA, Bañuelos C, Setlow B, Bizon JL (2016) Prefrontal cortical GABAergic signaling and impaired behavioral flexibility in aged F344 rats. Neuroscience.

Boccaletti S, Latora V, Moreno Y, Chavez M, Hwang DU (2006) Complex networks: Structure and dynamics. Physics Reports-Review Section of Physics Letters 424:175-308.

Bullmore E, Sporns O (2009) Complex brain networks: graph theoretical analysis of structural and functional systems. Nat Rev Neurosci 10:186-198.

Bullmore E, Sporns O (2012) The economy of brain network organization. Nat Rev Neurosci 13:336-349.

Burton AC, Nakamura K, Roesch MR (2015) From ventral-medial to dorsal-lateral striatum: neural correlates of reward-guided decision-making. Neurobiology of Learning and Memory 117:51-59.

Cao M, Wang JH, Dai ZJ, Cao XY, Jiang LL, Fan FM, Song XW, Xia MR, Shu N, Dong Q, Milham MP, Castellanos FX, Zuo XN, He Y (2014a) Topological organization of the human brain functional connectome across the lifespan. Dev Cogn Neurosci 7:76-93.

Cao W, Luo C, Zhu B, Zhang D, Dong L, Gong J, Gong D, He H, Tu S, Yin W, Li J, Chen H, Yao D (2014b) Resting-state functional connectivity in anterior cingulate cortex in normal aging. Front Aging Neurosci 6:280.

Carp J, Park J, Polk TA, Park DC (2011) Age differences in neural distinctiveness revealed by multi-voxel pattern analysis. Neuroimage 56:736-743.

Chadick JZ, Zanto TP, Gazzaley A (2014) Structural and functional differences in medial prefrontal cortex underlie distractibility and suppression deficits in ageing. Nat Commun 5:4223.

Chan MY, Park DC, Savalia NK, Petersen SE, Wig GS (2014) Decreased segregation of brain systems across the healthy adult lifespan. Proceedings of the National Academy of Sciences 111:E4997-E5006.

Cole AJ, Saffen DW, Baraban JM, Worley PF (1989) Rapid increase of an immediate early gene messenger RNA in hippocampal neurons by synaptic NMDA receptor activation. Nature 340:474-476.

Colon-Perez LM, Tran K, Thompson K, Pace MC, Blum K, Goldberger BA, Gold MS, Bruijnzeel AW, Setlow B, Febo M (2016a) The Psychoactive Designer Drug and Bath Salt Constituent MDPV Causes Widespread Disruption of Brain Functional Connectivity. Neuropsychopharmacology.

Colon-Perez LM, Tran K, Thompson K, Pace MC, Blum K, Goldberger BA, Gold MS, Bruijnzeel AW, Setlow B, Febo M (2016b) The Psychoactive Designer Drug and Bath Salt Constituent MDPV Causes Widespread Disruption of Brain Functional Connectivity. Neuropsychopharmacology 41:2352-2365.

Colon-Perez LM, Ibanez KR, Suarez M, Torroella K, Acuna K, Ofori E, Levites Y, Vaillancourt DE, Golde TE, Chakrabarty P, Febo M (2019) Neurite orientation dispersion and density imaging reveals white matter and hippocampal microstructure changes produced by Interleukin-6 in the TgCRND8 mouse model of amyloidosis. Neuroimage 202:116138.

Colon-Perez LM, Pino JA, Saha K, Pompilus M, Kaplitz S, Choudhury N, Jagnarine DA, Geste JR, Levin BA, Wilks I, Setlow B, Bruijnzeel AW, Khoshbouei H, Torres GE, Febo M (2018) Functional connectivity, behavioral and dopaminergic alterations 24 hours following acute exposure to synthetic bath salt drug methylenedioxypyrovalerone. Neuropharmacology 137:178-193.

Cox RW (1996) AFNI: software for analysis and visualization of functional magnetic resonance neuroimages. Computers and biomedical research, an international journal 29:162-173.

Egimendia A, Minassian A, Diedenhofen M, Wiedermann D, Ramos-Cabrer P, Hoehn M (2019) Aging reduces the functional brain networks strength–a resting state fMRI study of healthy mouse brain. Frontiers in aging neuroscience 11:277.

Fandakova Y, Lindenberger U, Shing YL (2014) Deficits in process-specific prefrontal and hippocampal activations contribute to adult age differences in episodic memory interference. Cereb Cortex 24:1832-1844.

Febo M, Ferris CF (2014) Oxytocin and vasopressin modulation of the neural correlates of motivation and emotion: results from functional MRI studies in awake rats. Brain Res.

Febo M, Shields J, Ferris CF, King JA (2009) Oxytocin modulates unconditioned fear response in lactating dams: an fMRI study. Brain Res 1302:183-193.

Fillinger C, Yalcin I, Barrot M, Veinante P (2018) Efferents of anterior cingulate areas 24a and 24b and midcingulate areas 24a' and 24b' in the mouse. Brain Struct Funct 223:1747-1778.

Gabbott PL, Warner TA, Jays PR, Salway P, Busby SJ (2005) Prefrontal cortex in the rat: projections to subcortical autonomic, motor, and limbic centers. J Comp Neurol 492:145-177.

Geerligs L, Renken RJ, Saliasi E, Maurits NM, Lorist MM (2014) A Brain-Wide Study of Age-Related Changes in Functional Connectivity. Cerebral Cortex 25:1987-1999.

Gefen T, Peterson M, Papastefan ST, Martersteck A, Whitney K, Rademaker A, Bigio EH, Weintraub S, Rogalski E, Mesulam MM, Geula C (2015) Morphometric and histologic substrates of cingulate integrity in elders with exceptional memory capacity. J Neurosci 35:1781-1791.

Gerrard JL, Burke SN, McNaughton BL, Barnes CA (2008) Sequence reactivation in the hippocampus is impaired in aged rats. J Neurosci 28:7883-7890.

Gold PE (2004) Coordination of multiple memory systems. Neurobiol Learn Mem 82:230-242.

Goyal MS, Vlassenko AG, Blazey TM, Su Y, Couture LE, Durbin TJ, Bateman RJ, Benzinger TL, Morris JC, Raichle ME (2017) Loss of Brain Aerobic Glycolysis in Normal Human Aging. Cell Metab 26:353-360.e353.

Grady C (2012) The cognitive neuroscience of ageing. Nat Rev Neurosci 13:491-505.

Grady C, Sarraf S, Saverino C, Campbell K (2016) Age differences in the functional interactions among the default, frontoparietal control, and dorsal attention networks. Neurobiol Aging 41:159-172.

Gray DT, Smith AC, Burke SN, Gazzaley A, Barnes CA (2017) Attentional updating and monitoring and affective shifting are impacted independently by aging in macaque monkeys. Behav Brain Res 322:329-338.

Graybiel AM (1998) The basal ganglia and chunking of action repertoires. Neurobiol Learn Mem 70:119-136.

Gremel CM, Costa RM (2013) Orbitofrontal and striatal circuits dynamically encode the shift between goal-directed and habitual actions. Nature communications 4:2264.

Guzowski JF, McNaughton BL, Barnes CA, Worley PF (1999) Environment-specific expression of the immediate-early gene Arc in hippocampal neuronal ensembles. Nat Neurosci 2:1120-1124.

Hernandez AR, Maurer AP, Reasor JE, Turner SM, Barthle SE, Johnson SA, Burke SN (2015) Age-related impairments in object-place associations are not due to hippocampal dysfunction. Behav Neurosci 129:599-610.

Hernandez AR, Reasor JE, Truckenbrod LM, Lubke KN, Johnson SA, Bizon JL, Maurer AP, Burke SN (2017) Medial prefrontal-perirhinal cortical communication is necessary for flexible response selection. Neurobiol Learn Mem 137:36-47.

Hernandez AR, Hernandez CM, Campos KT, Truckenbrod LM, Sakarya Y, McQuail JA, Carter CS, Bizon JL, Maurer AP, Burke SN (2018a) The Antiepileptic Ketogenic Diet Alters Hippocampal Transporter Levels and Reduces Adiposity in Aged Rats. J Gerontol A Biol Sci Med Sci 73:450-458.

Hernandez AR, Reasor JE, Truckenbrod LM, Campos KT, Federico QP, Fertal KE, Lubke KN, Johnson SA, Clark BJ, Maurer AP, Burke SN (2018b) Dissociable effects of advanced age on prefrontal cortical and medial temporal lobe ensemble activity. Neurobiol Aging 70:217-232.

Hoffman P, Morcom AM (2018) Age-related changes in the neural networks supporting semantic cognition: A meta-analysis of 47 functional neuroimaging studies. Neurosci Biobehav Rev 84:134-150.

Insel N, Barnes CA (2015) Differential Activation of Fast-Spiking and Regular-Firing Neuron Populations During Movement and Reward in the Dorsal Medial Frontal Cortex. Cereb Cortex 25:2631-2647.

Insel N, Patron LA, Hoang LT, Nematollahi S, Schimanski LA, Lipa P, Barnes CA (2012) Reduced gamma frequency in the medial frontal cortex of aged rats during behavior and rest: implications for age-related behavioral slowing. J Neurosci 32:16331-16344.

Iordan AD, Cooke KA, Moored KD, Katz B, Buschkuehl M, Jaeggi SM, Jonides J, Peltier SJ, Polk TA, Reuter-Lorenz PA (2017) Aging and Network Properties: Stability Over Time and Links with Learning during Working Memory Training. Front Aging Neurosci 9:419.

Jenkinson M, Bannister P, Brady M, Smith S (2002) Improved optimization for the robust and accurate linear registration and motion correction of brain images. NeuroImage 17:825-841.

Jo YS, Lee I (2010) Disconnection of the hippocampal-perirhinal cortical circuits severely disrupts object-place paired associative memory. The Journal of neuroscience : the official journal of the Society for Neuroscience 30:9850-9858.

Johnson SA, Turner SM, Santacroce LA, Bizon JL, Maurer AP, Burke SN (2017a) Age-related impairments in discriminating perceptually similar objects parallel those observed in humans. Accepted, *Hippocampus*.

Johnson SA, Turner SM, Santacroce LA, Carty KN, Shafiq L, Bizon JL, Maurer AP, Burke SN (2017b) Rodent age-related impairments in discriminating perceptually similar objects parallel those observed in humans. Hippocampus 27:759-776.

Kaiser M, Hilgetag CC (2006) Nonoptimal component placement, but short processing paths, due to long-distance projections in neural systems. PLoS Comput Biol 2:e95.

Kannurpatti SS, Biswal BB, Kim YR, Rosen BR (2008) Spatio-temporal characteristics of low-frequency BOLD signal fluctuations in isoflurane-anesthetized rat brain. Neuroimage 40:1738-1747.

960 Kennedy KM, Boylan MA, Rieck JR, Foster CM, Rodrigue KM (2017) Dynamic range in BOLD
961 modulation: lifespan aging trajectories and association with performance. Neurobiol
962 Aging 60:153-163.
963 Kim T, Masamoto K, Fukuda M, Vazquez A, Kim SG (2010) Frequency-dependent neural
964 activity, CBF, and BOLD fMRI to somatosensory stimuli in isoflurane-anesthetized rats.
965 Neuroimage 52:224-233.
966 LaClair M, Febo M, Nephew B, Gervais NJ, Poirier G, Workman K, Chumachenko S, Payne L,
967 Moore MC, King JA, Lacreuse A (2019) Sex Differences in Cognitive Flexibility and
968 Resting Brain Networks in Middle-Aged Marmosets. eNeuro 6.
969 Lee I, Byeon JS (2014) Learning-dependent Changes in the Neuronal Correlates of Response
970 Inhibition in the Prefrontal Cortex and Hippocampus. Exp Neurobiol 23:178-189.
971 Liang X, Hsu LM, Lu H, Sumiyoshi A, He Y, Yang Y (2018) The Rich-Club Organization in Rat
972 Functional Brain Network to Balance Between Communication Cost and Efficiency.
973 Cerebral cortex (New York, NY : 1991) 28:924-935.
974 Lockhart SN, DeCarli C (2014) Structural imaging measures of brain aging. Neuropsychol Rev
975 24:271-289.
976 Masamoto K, Kim T, Fukuda M, Wang P, Kim SG (2007) Relationship between neural, vascular,
977 and BOLD signals in isoflurane-anesthetized rat somatosensory cortex. Cereb Cortex
978 17:942-950.
979 McQuail JA, Nicolle MM (2015) Spatial reference memory in normal aging Fischer 344 x Brown
980 Norway F1 hybrid rats. Neurobiol Aging 36:323-333.
981 Morcom AM, Henson RNA (2018) Increased Prefrontal Activity with Aging Reflects Nonspecific
982 Neural Responses Rather than Compensation. J Neurosci 38:7303-7313.
983 Nasrallah FA, To XV, Chen D-Y, Routtenberg A, Chuang K-H (2016) Functional connectivity
984 MRI tracks memory networks after maze learning in rodents. Neuroimage 127:196-202.
985 Nephew BC, Caffrey MK, Felix-Ortiz AC, Ferris CF, Febo M (2009) Blood oxygen level-
986 dependent signal responses in corticolimbic 'emotions' circuitry of lactating rats facing
987 intruder threat to pups. Eur J Neurosci 30:934-945.
988 Nephew BC, Febo M, Huang W, Colon-Perez LM, Payne L, Poirier GL, Greene O, King JA
989 (2018) Early life social stress and resting state functional connectivity in postpartum rat
990 anterior cingulate circuits. J Affect Disord 229:213-223.
991 Newman MEJ (2003) The Structure and Function of Complex Networks. SIAM Review 45:167-
992 256.
993 Nicolle MM, Baxter MG (2003) Glutamate receptor binding in the frontal cortex and dorsal
994 striatum of aged rats with impaired attentional set-shifting. Eur J Neurosci 18:3335-3342.
995 Nieves-Martinez E, Haynes K, Childers SR, Sonntag WE, Nicolle MM (2012) Muscarinic
996 receptor/G-protein coupling is reduced in the dorsomedial striatum of cognitively
997 impaired aged rats. Behav Brain Res 227:258-264.
998 Nyberg L (2017) Functional brain imaging of episodic memory decline in ageing. J Intern Med
999 281:65-74.
1000 Nyberg L, Lovden M, Riklund K, Lindenberger U, Backman L (2012) Memory aging and brain
1001 maintenance. Trends Cogn Sci 16:292-305.
1002 Orsini CA, Colon-Perez LM, Heshmati SC, Setlow B, Febo M (2018) Functional Connectivity of
1003 Chronic Cocaine Use Reveals Progressive Neuroadaptations in Neocortical, Striatal,
1004 and Limbic Networks. eNeuro 5.
1005 Packard MG, McGaugh JL (1992) Double dissociation of fornix and caudate nucleus lesions on
1006 acquisition of two water maze tasks: further evidence for multiple memory systems.
1007 Behav Neurosci 106:439-446.
1008 Park DC, Polk TA, Park R, Minear M, Savage A, Smith MR (2004) Aging reduces neural
1009 specialization in ventral visual cortex. Proc Natl Acad Sci U S A 101:13091-13095.

1010 Paxinos G, Watson C (1998) The Rat Brain in Stereotaxic Coordinates, 4 Edition. San Diego:
1011 Academic Press.
1012 Pooters T, Laeremans A, Gantois I, Vermaercke B, Arckens L, D'Hooge R (2017) Comparison
1013 of the spatial-cognitive functions of dorsomedial striatum and anterior cingulate cortex in
1014 mice. PLoS One 12:e0176295.
1015 Pych JC, Chang Q, Colon-Rivera C, Haag R, Gold PE (2005) Acetylcholine release in the
1016 hippocampus and striatum during place and response training. Learn Mem 12:564-572.
1017 Regier PS, Amemiya S, Redish AD (2015) Decision making: neural mechanisms: hippocampus
1018 and subregions of the dorsal striatum respond differently to a behavioral strategy change
1019 on a spatial navigation task. Journal of Neurophysiology 114:1399.
1020 Reuter-Lorenz PA, Cappell KA (2008) Neurocognitive aging and the compensation hypothesis.
1021 Current directions in psychological science 17:177-182.
1022 Riehl JR, Palanca BJ, Ching S (2018) High-energy brain dynamics during anesthesia-induced
1023 unconsciousness. Netw Neurosci 1:431-445.
1024 Rogalski E, Stebbins GT, Barnes CA, Murphy CM, Stoub TR, George S, Ferrari C, Shah RC,
1025 deToledo-Morrell L (2012) Age-related changes in parahippocampal white matter
1026 integrity: a diffusion tensor imaging study. Neuropsychologia 50:1759-1765.
1027 Rubinov M, Sporns O (2010) Complex network measures of brain connectivity: uses and
1028 interpretations. NeuroImage 52:1059-1069.
1029 Sala-Llonch R, Bartrés-Faz D, Junqué C (2015a) Reorganization of brain networks in aging: a
1030 review of functional connectivity studies. Front Psychol 6:663.
1031 Sala-Llonch R, Bartres-Faz D, Junque C (2015b) Reorganization of brain networks in aging: a
1032 review of functional connectivity studies. Frontiers in psychology 6:663.
1033 Sala-Llonch R, Junque C, Arenaza-Urquijo EM, Vidal-Pineiro D, Valls-Pedret C, Palacios EM,
1034 Domenech S, Salva A, Bargallo N, Bartres-Faz D (2014) Changes in whole-brain
1035 functional networks and memory performance in aging. Neurobiol Aging.
1036 Salami A, Pudas S, Nyberg L (2014) Elevated hippocampal resting-state connectivity underlies
1037 deficient neurocognitive function in aging. Proc Natl Acad Sci U S A 111:17654-17659.
1038 Samson RD, Barnes CA (2013) Impact of aging brain circuits on cognition. Eur J Neurosci
1039 37:1903-1915.
1040 Saramaki J, Kivel M, Onnela J-P, Kaski K, Kertesz J (2007) Generalizations of the clustering
1041 coefficient to weighted complex networks. Physical Review E 75:027105.
1042 Steward O, Wallace CS, Lyford GL, Worley PF (1998) Synaptic activation causes the mRNA for
1043 the IEG Arc to localize selectively near activated postsynaptic sites on dendrites. Neuron
1044 21:741-751.
1045 Takeuchi H, Taki Y, Nouchi R, Sekiguchi A, Kotozaki Y, Nakagawa S, Makoto Miyauchi C,
1046 Sassa Y, Kawashima R (2017) Neural plasticity in amplitude of low frequency
1047 fluctuation, cortical hub construction, regional homogeneity resulting from working
1048 memory training. Sci Rep 7:1470.
1049 Tomas Pereira I, Gallagher M, Rapp PR (2015) Head west or left, east or right: interactions
1050 between memory systems in neurocognitive aging. Neurobiology of aging 36:3067-3078.
1051 Turturro A, Witt WW, Lewis S, Hass BS, Lipman RD, Hart RW (1999) Growth curves and
1052 survival characteristics of the animals used in the Biomarkers of Aging Program. J
1053 Gerontol A Biol Sci Med Sci 54:B492-501.
1054 Vaidya JG, Paradiso S, Boles Ponto LL, McCormick LM, Robinson RG (2007) Aging, grey
1055 matter, and blood flow in the anterior cingulate cortex. Neuroimage 37:1346-1353.
1056 van den Heuvel MP, Kahn RS, Goni J, Sporns O (2012) High-cost, high-capacity backbone for
1057 global brain communication. Proc Natl Acad Sci U S A 109:11372-11377.
1058 Vazdarjanova A, Guzowski JF (2004) Differences in hippocampal neuronal population
1059 responses to modifications of an environmental context: evidence for distinct, yet
1060 complementary, functions of CA3 and CA1 ensembles. J Neurosci 24:6489-6496.

1061 Vazdarjanova A, Ramirez-Amaya V, Insel N, Plummer TK, Rosi S, Chowdhury S, Mikhael D,
1062 Worley PF, Guzowski JF, Barnes CA (2006) Spatial exploration induces ARC, a
1063 plasticity-related immediate-early gene, only in calcium/calmodulin-dependent protein
1064 kinase II-positive principal excitatory and inhibitory neurons of the rat forebrain. J Comp
1065 Neurol 498:317-329.
1066 Vertes RP, Hoover WB, Rodriguez JJ (2012) Projections of the central medial nucleus of the
1067 thalamus in the rat: node in cortical, striatal and limbic forebrain circuitry. Neuroscience
1068 219:120-136.
1069 Williams KA, Magnuson M, Majeed W, LaConte SM, Peltier SJ, Hu X, Keilholz SD (2010)
1070 Comparison of alpha-chloralose, medetomidine and isoflurane anesthesia for functional
1071 connectivity mapping in the rat. Magn Reson Imaging 28:995-1003.
1072 Xia M, Wang J, He Y (2013) BrainNet Viewer: a network visualization tool for human brain
1073 connectomics. PloS one 8:e68910.
1074 Yee JR, Kenkel W, Caccaviello JC, Gamber K, Simmons P, Nedelman M, Kulkarni P, Ferris CF
1075 (2015) Identifying the integrated neural networks involved in capsaicin-induced pain
1076 using fMRI in awake TRPV1 knockout and wild-type rats. Front Syst Neurosci 9:15.
1077 Yoshizawa H, Gazes Y, Stern Y, Miyata Y, Uchiyama S (2014) Characterizing the normative
1078 profile of 18F-FDG PET brain imaging: sex difference, aging effect, and cognitive
1079 reserve. Psychiatry Res 221:78-85.
1080

1081

Figure Legends

Figure 1. Working memory/biconditional association task (WM/BAT) performance. (a) Schematic of the WM/BAT. Rats began testing by being placed at the location labeled 'start', facing away from the choice platforms and began traversing the continuous-T maze maze alternating between left and right turns. After turning, before returning to the central stem, rats solved an object discrimination problem in which the correct choice (green check) was contingent on side of the maze. On the left, the owl is rewarded and on the right the dog is rewarded. The position of the objects over the well in a choice platform varied across trials. **(b)** Performance on WM/BAT over days of testing task in young (black) and aged (grey) rats between resting state scans. **(c)** After the third scan, rats were re-trained on WM/BAT with different objects for 13 days before performing the task a final time, followed by immediate sacrifice to label the mRNA products of the activity-dependent immediate-early gene Arc. **(d)** The average number of working memory errors (making two turns in the same direction rather than alternating) per day of testing in young and aged rats. The incidence of working memory errors decreased over testing, but did not differ by age. Error bars are ± 1 SEM, *p < 0.05.

Figure 2. Response Biases during WM/BAT training. (a) The response bias index quantifies a rat's tendency to select an object on one side (left vs right) regardless of the object identity and choice platform on the maze. A value of 0 is no bias and a value of 1 is a complete bias to one side. Most rats show a response bias that decreases as they start to perform better. Aged rats have a tendency to retain a response bias across more days of testing. The response bias is plotted across testing days between resting state fMRI scans. **(b)** Shows the response bias across days of testing before and on the day of the *Arc* experiment. Overall, the aged rats showed a significantly greater response bias than the young rats. **(c)** The response bias of young and aged rats on the day immediately following the baseline scan, the days prior to scans 2 and 3, and on the day of the Arc experiment. Aged rats had a significantly greater response bias compared to young rats prior to scan. Error bars are ± 1 SEM, *p < 0.05.

Figure 3. Connectivity patterns by scanning session and age group. Connected modules with edges z > 0.3 for young **(a)** and aged **(b)** rats across scan sessions. Connectivity indices indicate larger network engagement between baseline and the second and third scanning sessions in aged (blue arrow), but not young rats. This is indicated by more nodes with node strength > 15 **(c)** and degree > 40 **(d)**.

Figure 4. Nodes with increased strength. 16 nodes with strength > 15 during scan 2 in aged rats were identified from the distribution shown in Figure 1. Connectivity patterns of these nodes for the young **(a)** and aged **(b)** groups. The table in **(c)** lists the regions by hemisphere that correspond to these nodes.

Figure 5. Seed analysis of ACC connectivity. (a) Connectivity with ACC in young (left) and aged (right) rats as a function of scan session. The insets on the left show the locations of the ACC (green shaded) and dorsal striatum (purple shaded) for bregma locations anterior to posterior +2 to -1.8. **(b)** Connectivity between the ACC and DS as a function of scan session for the lateral (left) and medial (right) subregions in young (black) and aged (grey) rats. The main effects of scan session ($F_{[2,64]} = 1.69$; $p = 0.19$), age ($F_{[1,32]} = 3.67$; $p = 0.07$) and subregion of the striatum ($F_{[1,32]} = 1.15$; $p = 0.29$) did not reach statistical significance. The interaction effect between age and scan session was significant, however ($F_{[2,64]} = 3.75$; $p = 0.03$). Post hoc analysis indicated that there were no significant age differences between ACC-DS connectivity during the baseline scan ($p = 0.63$), and scan 2 ($p = 0.26$), but the aged rats had significantly higher connectivity relative to young during the third scan ($p = 0.004$). Error bars are ± 1 SEM, *$p < 0.05$.

Figure 6: Response bias and ACC-DS connectivity. Across the 3 scanning sessions, the mean response bias of individual rats measured during behavior significantly correlated with ACC-DS connectivity ($R_{[29]} = 0.48$, $p = 0.008$), such that more connectivity corresponded with a higher proportion of trials in which this aberrant strategy was used. Dashed lines indicate line of best fit for young (black) and aged (grey) rats.

Figure 7. Rich club organization increases with cognitive training in aged rats. (a) Top figure, rich club participation index between young and aged rats, at the baseline scan (shaded area $K > 27$ and $p < 0.05$), bottom figure shows the overall difference increase for between aged and young rats. **(b)** Top figure, young rats rich club participation index, and bottom is the difference between scanning sessions. No changes in any of the sessions or any K-level was observed. **(c)** Top figure, aged rats rich club participation in aged group increase following cognitive training for large K-levels (shaded area $K > 21$ and $p < 0.05$), bottom figure shows the overall difference increase for both sessions. Error bars are ± 1 SEM, and shaded regions indication $p < 0.05$.

Figure 8: Neuronal activation during WM/BAT and spatial alternation in young and aged rats. (a) A DAPI stained section showing regions that were sampled (top, white squares) within the anterior cingulate cortex (ACC). Bottom panels show representative *Arc* labeling (red) in a young (left) and an aged rat (right). **(b)** Percentage of *Arc* positive cells in the ACC corresponding to transcription during WM/BAT, or the alternation task in young (black) and ages (grey) rats. There was not a significant main effect of task, age, or an interaction effect on the *Arc* expression patterns. **(c)** A DAPI stained section showing regions within the DS that were sampled for analysis of *Arc* expression (top, white squares). Bottom panels show representative images labeled for *Arc* mRNA from a young (left) and an aged rat (right). **(d)** Percentage of *Arc* positive cells in the DS corresponding to transcription during WM/BAT, or the alternation task. The aged rats had significantly more cells that were positive for *Arc* compared to the young animals ($F_{[1,28]} = 5.58$, $p < 0.03$). The interaction effect between age and task was also significant ($F_{[1,28]} = 13.64$, $p < 0.001$), such that aged rats had more cells than young rats that transcribed *Arc* during WM/BAT ($p < 0.001$), but this same difference was not observed during the alternation task ($p = 0.43$). Error bars are ± 1 SEM, *$p < 0.05$.

Figure 9: Reward expectancy and population overlap in ACC and DS. (a) The average number of rewards received for young (black) and aged (grey) rats during the WM/BAT and control alternation task on the day of the *Arc* experiment. Rats received more rewards during the alternation task compared to WM/BAT ($F_{[1,7]} = 27.27$, $p = 0.001$). There was also a trend for aged rats to receive fewer rewards than young ($F_{[1,7]} = 5.55$, $p = 0.051$), and for this to interact with task ($F_{[1,7]} = 3.67$, $p = 0.097$). **(b)** The average similarity score for young (black) and aged (grey) rats in the ACC, DLS and DMS. The main effect of region was not significant ($F_{[2,14]} = 0.58$, $p = 0.57$). There was also not a significant main effect of age on similarity score ($F_{[1,7]} = 2.83$, $p = 0.14$), nor did the interaction effect between region and age reach statistical significance ($F_{[1,7]} = 0.15$, $p = 0.86$). Error bars are ± 1 SEM.

Figure 10. ACC-DS connectivity in untrained rats. In rats that were scanned for resting state connectivity longitudinally after 11 and 24 days of traversing a track for reward for 32 trials, there were no significant differences between ACC-DS connectivity in the lateral (left) and medial (right) subregions across scan session ($F_{[2,88]} = 0.39$, $p = 0.68$) or age group ($F_{[1,44]} = 0.57$, $p = 0.46$). Moreover, the interaction of age and scan was not significant ($F_{[2,88]} = 0.82$, $p =$

0.44). Finally, there was no effect of DS subregion ($F_{[1,44]} = 1.95$, $p = 0.17$) and none of the other interaction terms were statistically different ($P>0.1$ for all comparisons).

Figure 11. Rich club organization does not change in untrained rats. The rich club participation index in young (left) and aged (right) rats across the different scan sessions. Across longitudinal scans the rich club index did not change in either age group.

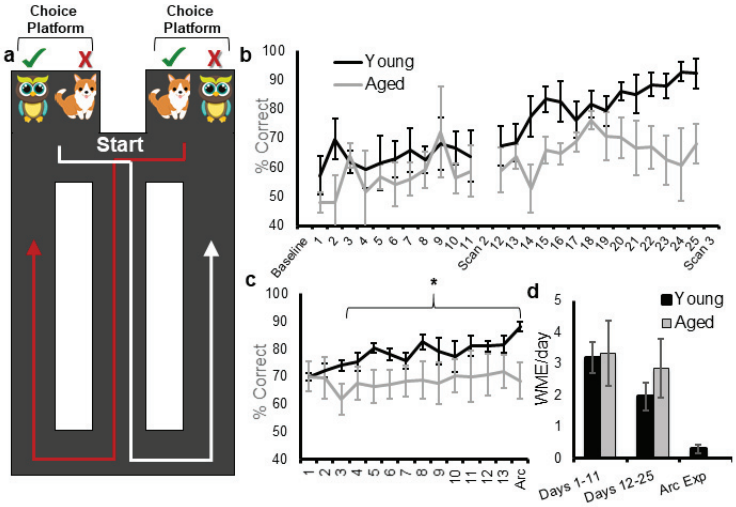

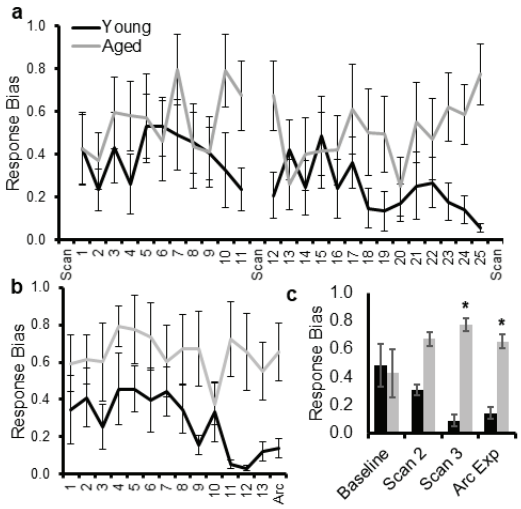

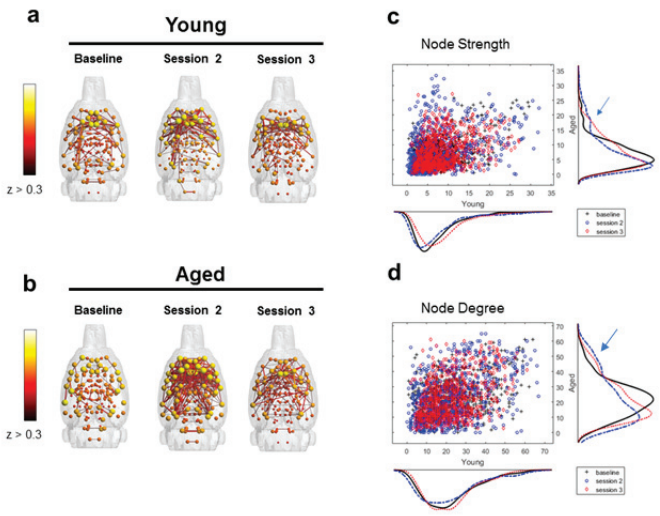

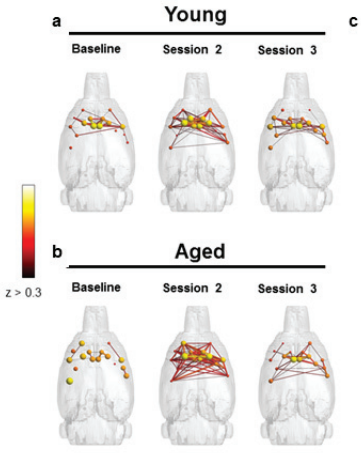

c

Left Hemisphere	Right Hemisphere
Anterior Cingulate	Anterior Cingulate
Insular Cortex	Insular Cortex
Lat. Orbital Cortex	Lat. Orbital Cortex
M1 Motor	M1 Motor
M2 Motor	M2 Motor
S1 SSC jaw	S1 SSC FL
S1 SSC BF	S1 SSC ul
Ventrolateral Striatum	S2 SSC